THE JOURNAL OF BIOLOGICAL CHEMISTRY VOL. 285, NO. 25, pp. 19002–19011, June 18, 2010
Printed in the U.S.A.

Transcriptional Regulation of Cannabinoid Receptor-1 Expression in the Liver by Retinoic Acid Acting via Retinoic Acid Receptor-γ*

Received for publication, September 21, 2009, and in revised form, April 19, 2010 Published, JBC Papers in Press, April 21, 2010, DOI 10.1074/jbc.M109.068460

Bani Mukhopadhyay[‡1], Jie Liu[‡], Douglas Osei-Hyiaman[‡], Grzegorz Godlewski[‡], Partha Mukhopadhyay[‡], Lei Wang[‡], Won-Il Jeong[‡], Bin Gao[‡], Gregg Duester[§], Ken Mackie[¶], Soichi Kojima[‖], and George Kunos[‡2]

From the [‡]Laboratory of Physiologic Studies, National Institute on Alcohol Abuse and Alcoholism, National Institutes of Health, Bethesda, Maryland 20892-9413, the [§]Sanford-Burnham Medical Research Institute, La Jolla, California 92037, the [¶]Gill Center for Biomolecular Science, Indiana University, Bloomington, Indiana 47405, and the [‖]Molecular Ligand Biology Research Team, Chemical Genomics Research Group, Chemical Biology Department, RIKEN Advanced Science Institute, Saitam 351-0198, Japan

Alcoholism can result in fatty liver that can progress to steatohepatitis, cirrhosis, and liver cancer. Mice fed alcohol develop fatty liver through endocannabinoid activation of hepatic CB_1 cannabinoid receptors (CB_1R), which increases lipogenesis and decreases fatty acid oxidation. Chronic alcohol feeding also up-regulates CB_1R in hepatocytes *in vivo*, which could be replicated *in vitro* by co-culturing control hepatocytes with hepatic stellate cells (HSC) isolated from ethanol-fed mice, implicating HSC-derived mediator(s) in the regulation of hepatic CB_1R (Jeong, W. I., Osei-Hyiaman, D., Park, O., Liu, J., Bátkai, S., Mukhopadhyay, P., Horiguchi, N., Harvey-White, J., Marsicano, G., Lutz, B., Gao, B., and Kunos, G. (2008) *Cell Metab.* 7, 227–235). HSC being a rich source of retinoic acid (RA), we tested whether RA and its receptors may regulate CB_1R expression in cultured mouse hepatocytes. Incubation of hepatocytes with RA or RA receptor (RAR) agonists increased CB_1R mRNA and protein, the most efficacious being the RARγ agonist CD437 and the pan-RAR agonist TTNPB. The endocannabinoid 2-arachidonoylglycerol (2-AG) also increased hepatic CB_1R expression, which was mediated indirectly via RA, because it was absent in hepatocytes from mice lacking retinaldehyde dehydrogenase 1, the enzyme catalyzing the generation of RA from retinaldehyde. The binding of RARγ to the CB_1R gene 5′ upstream domain in hepatocytes treated with RAR agonists or 2-AG was confirmed by chromatin immunoprecipitation and electrophoretic mobility shift and antibody supershift assays. Finally, TTNPB-induced CB_1R expression was attenuated by small interfering RNA knockdown of RARγ in hepatocytes. We conclude that RARγ regulates CB_1R expression and is thus involved in the control of hepatic fat metabolism by endocannabinoids.

The biological actions of endocannabinoids and their plant-derived and synthetic analogs are mediated by G protein-coupled cannabinoid receptors. Two cannabinoid receptors have been identified to date; CB_1R[3] are expressed at very high levels in the brain and at much lower concentrations in many peripheral tissues, whereas CB_2R are expressed primarily, although not exclusively, in cells of the immune and hematopoietic systems (2). Recent findings indicate that CB_1R are expressed at low yet functionally relevant levels in the liver, and their activation promotes *de novo* lipogenesis and inhibits fatty acid oxidation (3). Through these effects, endocannabinoids play a key role in the development of fatty liver in response to high fat diets (4) or chronic alcohol intake (1). In mice fed a liquid alcohol diet, the development of fatty liver was found to involve paracrine activation of hepatic CB_1R by hepatic stellate cell (HSC)-derived endocannabinoids. Chronic alcohol feeding also resulted in up-regulation of CB_1R in hepatocytes *in vivo*, which could be replicated *in vitro* by co-culturing control mouse hepatocytes with HSC isolated from ethanol-fed mice (1). This suggests that HSC-derived mediator(s) can regulate CB_1R expression in hepatocytes. HSC being the richest source of retinoic acid (RA) in the body, we examined the possible role of RA and its receptors in the regulation of CB_1R expression in mouse hepatocytes.

RA is generated *in vivo* by sequential oxidation of retinol (vitamin A), first through the action of alcohol dehydrogenase to yield retinaldehyde and then by retinaldehyde dehydrogenase (Raldh) to yield RA (5, 6). RA and its homologs are potent regulators of gene expression and play vital roles in a wide variety of biological functions, including cellular differentiation and proliferation, embryonic development, tissue repair, and immune functions (7, 8). The cellular effects of RA are mediated by RA receptors (RARs), which are ligand-activated tran-

* This work was supported, in whole or in part, by National Institutes of Health intramural funds from the National Institute on Alcohol Abuse and Alcoholism (to G. K.) and National Institute on Drug Abuse Grants DA11322 and DA21696 (to K. M.). This work was also supported by the Chemical Genomics Research Program from RIKEN (to S.K.).

This paper is dedicated by B.M. to the memory of her beloved father, Sridhar Mukherjee, who died during the course of this work.

[1] To whom correspondence may be addressed: National Institute on Alcohol Abuse and Alcoholism, 5625 Fishers Ln., MSC-9413, Bethesda, MD 20892-9413. Tel.: 301-443-2069; Fax: 301-480-0257; E-mail: mukhopadhyayb@mail.nih.gov.

[2] To whom correspondence may be addressed: National Institute on Alcohol Abuse and Alcoholism, 5625 Fishers Ln., MSC-9413, Bethesda, MD 20892-9413. Tel.: 301-443-2069; Fax: 301-480-0257; E-mail: gkunos@mail.nih.gov.

[3] The abbreviations used are: CB_1R and CB_2R, CB_1 and CB_2 cannabinoid receptor(s), respectively; TTNPB, 4-[(*E*)-2-(5,6,7,8-tetrahydro-5,5,8,8-tetramethyl-2-naphthalenyl)-1-propenyl]benzoic acid; CD437, 6-(4-hydroxy-3-tricyclo[3.3.1.13,7]dec-1-ylphenyl)-2-naphthalenecarboxylic acid; LE135, 4-(7,8,9,10-tetrahydro-5,7,7,10,10-pentamethyl-5H-benzo[e]naphtho[2,3-b][1,4]diazepin-13-yl)benzoic acid; HSC, hepatic stellate cells; RA, retinoic acid; Raldh, retinaldehyde dehydrogenase; 2-AG, 2-arachidonoylglycerol; BisTris, 2-[bis(2-hydroxyethyl)amino]-2-(hydroxymethyl)propane-1,3-diol; ChIP, chromatin immunoprecipitation; EMSA, electrophoretic mobility shift assay; siRNA, small interfering RNA.

scription factors. Receptors for RA consist of heterodimers of RAR and retinoid X receptors (RXR). The RAR and RXR each have at least three distinct isoforms encoded by separate genes: *RAR-α*, *-β*, and *-γ* and *RXR-α*, *-β*, and *-γ*, respectively (9). The RAR/RXR heterodimers bind to the appropriate response elements of RA target genes to exert a broad range of biological effects. RXR, whose cognate ligand is 9-*cis*-RA, also forms heterodimers with other nuclear receptors, such as peroxisome proliferation-activated receptor α or γ, thyroid hormone receptors, farnesoid X receptor, and liver X receptors (10, 11).

Particularly relevant to the present study is a recent observation that RA-dependent neuronal differentiation of mouse P19 pluripotent embryonic cancer cells was associated with a strong induction of CB_1R but not CB_2R. This effect may have been secondary to the process of neuronal differentiation or a direct effect of RA on CB_1R gene expression (12). To test whether RA is a direct transcriptional regulator of CB_1R expression, we have undertaken an analysis of the effect of RA and its analogs on CB_1R gene expression in a well differentiated, non-neuronal, primary cultured cell, the mouse hepatocyte. The results indicate that RA up-regulates CB_1R gene transcription in hepatocytes via binding to RARγ, which then binds to the 5′ upstream regulatory domain of the CB_1R gene to induce its transcription. The results further indicate that autoinduction of the hepatic CB_1R by the endocannabinoid 2-arachidonoylglycerol (2-AG) is also dependent on activation of this pathway.

EXPERIMENTAL PROCEDURES

Animals—All protocols were approved by the Institutional Animal Care and Use Committee and were performed in accordance with the National Institutes of Health Guide for the Care and Use of Laboratory Animals. C57BL/6J mice were purchased from Jackson Laboratories. Male mice 10–12 weeks of age were used in all experiments. $CB_1^{+/+}$ and $CB_1^{-/-}$ littermates were obtained by breeding heterozygotes that had been back-crossed to a C57BL/6J background, as described (13). Mice with hepatocyte-specific knock-out of CB_1R ($LCB_1^{-/-}$ mice) were generated as described (1). $Raldh1^{-/-}$ mice on a mixed 129/C57Bl/6 background were generated as described (14). All experiments with knock-out mice used the corresponding homozygous wild-type (+/+) littermates as controls. Genotyping by PCR for the *Cre* transgene was performed as described previously (15). Individually caged mice were placed on a Lieber-DeCarli low fat liquid diet (Dyets) containing 1 kcal/ml, of which 18% was derived from protein, 12% from fat, and either 70% from carbohydrate (control diet) or 43% from carbohydrate and 27% from ethanol (ethanol diet). Mice had free access to the diet, and food intake and body weight were monitored daily. The mice were on these diets for a total of 30 days; ethanol was introduced gradually by increasing the content by 1% (v/v) each day until the mice were consuming a diet containing 5% (v/v) ethanol, which was then continued for 3 more weeks. For diet-induced obesity studies, a high fat diet with 60% of calories derived from fat (D12492, Research Diets) was fed to the mice for 14–16 weeks as described earlier (3, 16). At the end of this period, mice were sacrificed, and liver tissue and trunk blood were collected.

Reagents—The RARγ agonist CD437 was from Sigma, and the panagonist TTNPB was from Biomol. SR141716 (Rimonabant) had been provided from the National Institute of Drug Abuse Drug Supply Program. 2-AG was purchased from Tocris Bioscience (Ellisville, MO). All-*trans*-retinoic acid was from Sigma. RARα agonist AM580 was from Biomol. RARβ agonist CD2019 and RARβ antagonist LE135 were from Dr. Kagechika and CIRD Galderma Sophia Antipolis (Valbonne, France), respectively. Antibodies used were anti-actin monoclonal antibody (Chemicon), anti-RARγ monoclonal antibody, anti-RARα, and anti-RARβ (Abcam). A polyclonal antibody against the N-terminal region of the rat CB_1R was obtained from Cayman Chemicals. A rabbit polyclonal antibody against the last 15 amino acids of the C terminus of CB_1R (17) was also used to identify CB_1R in immunoprecipitates generated with the N-terminal antibody. RARγ protein was purchased from ProteinOne.

Isolation and Culture of Pure Fractions of Hepatocytes—Hepatocytes were isolated by collagenase perfusion of liver and then separated from nonparenchymal cells using Percoll (GE Healthcare) density gradient centrifugation (18). Hepatocytes were grown in Hepato-Zyme-SFM medium containing 10% fetal bovine serum, gentamycin, and L-glutamine (Invitrogen) in a CO_2 incubator at 37 °C with 5% CO_2 in air. Hepatocytes were freshly isolated and maintained under serum-deprived conditions for 24 h before treatments. Compounds were dissolved in DMSO and diluted in serum-free medium before being added to cultures. Matched dilutions of DMSO were used as vehicle controls.

Blood Chemistry—Serum alanine aminotransferase, aspartate aminotransferase, and ethanol levels were assayed using kits from Drew Scientific and BioAssay Systems, respectively. Blood ethanol levels were measured in blood drawn via tail clips at 8 a.m. (1).

Tissue Levels of Lipids—For measuring triglyceride and cholesterol levels in liver, mice were sacrificed, and their livers were removed and extracted. Total hepatic triglyceride and cholesterol were measured as described (19).

Real-time PCR Analyses—Total RNA was isolated from liver homogenate or from purified hepatocyte fractions using TRIzol reagents (Invitrogen) according to the manufacturer's instructions. The isolated RNA was treated with RNase-free DNase (Ambion) to remove traces of genomic DNA contamination. One μg of total RNA was reverse-transcribed to cDNA using Super-Script II (Invitrogen). The target gene expression was quantified with gene-specific primers and Power SYBR Green master mix (ABI) using a 7500 Realtime PCR instrument (Applied Biosystems). Each amplified sample was analyzed for homogeneity using dissociation curve analysis. Relative quantification was performed using the comparative C_T method (20). Primers used for mouse and human hepatocytes are listed in Table 1.

Western Blot Analyses—Protein was extracted from hepatocyte homogenate using T-PER lysis buffer (Pierce) containing protease inhibitor mixture set III and phosphatase inhibitor mixture set I (Calbiochem). Equal amounts (10 or 25 μg/lane) were fractionated on a Criterion 4–12% BisTris gel (Bio-Rad)

TABLE 1
Primers used for mouse and human hepatocytes

Gene	DNA sequence	Species
CB I (ChIP)	5′-AGGTAGCTGAGGACTGGAGGC-3′ 5′-AGCGTGGTCCCATCACGTGTTAAT-3′	Mouse
β-Actin (ChIP)	5′-TCGATATCCACGTGACATCCA-3′ 5′-AAATGCTGCACTGTGCGGCG-3′	Mouse
CB 1	5′-GTACCATCACCACAGACCTCCTC-3′ 5′-GGATTCAGAATCATGAAGCATCCA-3′	Mouse
Fas	5′-CATGACCTCGTGATGAACGTG-3′ 5′-GGTGAGGACGTTTACAAAGGC-3′	Mouse
RARγ	5′-GTTTACACCCTGGAAATGACCC-3′ 5′-GCAGGAATCTTATTTGGCAGC-3′	Mouse
SREBP-1c	5′-GCCCACAATGCCATTGAGA-3′ 5′-TGCTTGAGCTTCTGGTTGCTG-3′	Mouse
β-Actin	5′-TGCACCACCAACTGCTTAG-3′ 5′-GGATGCAGGGATGATGTTC-3′	Mouse
CB 1	5′-TTCCCTCTTGTGAAGGCACTG-3′ 5′-TCTTGACCGTGCTCTTGATGC-3′	Human
R-actin	5′-ATTGCCGACAGGATGCAGAAG-3′ 5′-TAGAAGCATTTGCGGTGGACG-3′	Human

and transferred onto nitrocellulose membrane using a semidry transfer apparatus (Bio-Rad). Blocking was done for 2 h in 5% nonfat dry milk in phosphate-buffered saline. The primary antibodies were added as per the manufacturer's recommended dilution in the blocking buffer containing 0.1% Tween 20 overnight at 4 °C. After three washes in phosphate-buffered saline containing 0.1% Tween 20, secondary horseradish peroxidase conjugate (PerkinElmer Life Sciences) was added, followed by three washes with phosphate-buffered saline containing 0.1% Tween 20. The blots were detected with Supersignal West Pico chemiluminescent substrate (Pierce) and developed using Eastman Kodak Co. Biomax film (PerkinElmer Life Sciences). Autoradiograms of Western blots were scanned and quantified using Quantity One software (Bio-Rad). All blots were normalized to the loading control β-actin (21).

CB_1R Immunoprecipitation—In some experiments, weak nonspecific bands in Western blots for CB_1R could be eliminated by first immunoprecipitating the cell extract using the CB_1R N-terminal antibody and then blotting the precipitated proteins using a different, C-terminal CB_1R antibody. CB_1R immunoprecipitation was carried out using Dynabeads® Protein G magnetic separation according to the manufacturer's protocol with minor modifications. Briefly, Dyna magnetic beads were washed and incubated with CB_1R N-terminal polyclonal antibody (Cayman Chemicals) for 3 h at 4 °C. After repeated washing of the Dynabeads-antibody complex, protein lysates from hepatocytes (100 μg for each sample) were added to the complex and incubated overnight at 4 °C. The Dynabeads-antibody-antigen complex was washed three times and eluted in 50 μl of NuPAGE LDS sample buffer/NuPAGE reducing agent mix and incubated for 10 min at 70 °C. Samples were loaded onto a Bio-Rad Criterion gel, and Western blotting was performed using the CB_1R C-terminal antibody.

Chromatin Immunoprecipitation (ChIP) Assay—ChIP assays were performed as described (22). Briefly, isolated hepatocytes were grown to confluence. After treatment as detailed in the figure legend (Fig. 7), cells were washed twice with phosphate-buffered saline and cross-linked with 1% formaldehyde at room temperature for 10 min. The cross-linking was stopped by adding 0.125 M glycine. Cells were washed two times with ice-cold phosphate-buffered saline and then resuspended in 0.3 ml of Farnham lysis buffer (0.5% Nonidet P-40, 85 mM KCl, 5 mM HEPES, pH 8.0, 1× protease inhibitor mixture (Roche Applied Science)) and sonicated, followed by centrifugation for 15 min. Supernatants were collected, and immunoprecipitation was performed at 4 °C.

First, the primary monoclonal antibody against RARγ (Santa Cruz Biotechnology, Inc., Santa Cruz, CA) was coupled to magnetic beads (Dynal beads, Invitrogen). The magnetic bead slurry was resuspended, washed three times and mixed with primary monoclonal antibody to RARγ in a rotator overnight at 4 °C. After that, coupled antibody was added to each chromatin preparation (after sonication) and incubated at 4 °C overnight on a rotator. Beads containing immunobound chromatins were collected by placing the microcentrifuge tubes on the magnet stand. Supernatants were discarded, and beads were washed with LiCl Wash Buffer (100 mM Tris-HCl, pH 7.5, 500 mM LiCl, 1% Nonidet P-40, 1% deoxycholate). The bead pellet was resuspended in 200 μl of IP Elution Buffer (1% SDS, 0.1 M $NaHCO_3$) by vortexing. Eluates and control lysates without immunoprecipitation (for input DNA) were pooled and heated at 65 °C overnight to reverse the formaldehyde cross-linking. DNA fragments were purified with a QIAquick spin kit (Qiagen). For PCR, 1-μl aliquots from a 50-μl DNA extract were subjected to 30–35 cycles of amplification. PCR amplification was carried out for the CB_1R promoter sequence.

CHIP DNA samples were also analyzed by real-time PCR using the ABI 7500 SYBR Green method and the same set of primers. The data were analyzed using the "-fold enrichment" method and mock IgG (for immunoprecipitation of DNA) as control (23).

Electrophoretic Mobility Shift Assay (EMSA)—Nuclear proteins (20 μg) were extracted with NE-PER nuclear extraction reagents (Pierce), and EMSA was performed with a LightShift chemiluminescent EMSA kit (Pierce). For EMSA, the binding reactions were performed for 20 min in 1× binding buffer, 5 mM $MgCl_2$, 50 ng/μl poly(dI-dC)(dI-dC), 0.05% Nonidet P-40, 2.5% glycerol, biotin 5′-end-labeled PCR amplicon, and RARγ or nuclear protein extracts, as described in the figure legends (Fig. 6). Purified recombinant RARγ protein was from ProteinOne (Bethesda, MD). RARγ was expressed as a His-tagged protein in the baculovirus system and purified by a combination of affinity and gel filtration chromatography (ProteinOne).

Samples were electrophoresed on a native 6% polyacrylamide gel in 1× Tris-borate-EDTA buffer and then transferred to a Biodyne membrane according to the manufacturer's recommendation. The retarded bands were detected by chemiluminescence using the LightShift Chemiluminescent EMSA kit. To confirm the identity of RARγ binding, supershift experiments were performed using the same samples with 1 μg of anti-RARγ antibody. For the competitive binding assay, non-labeled probe was added to the binding reaction at a 200-fold excess over the labeled probe.

RNA Interference Assay—For knockdown of RARγ, predesigned small interfering RNA (siRNA) reagents were obtained using an Accell SMARTpool siRNA kit (Dharmacon), following the manufacturer's recommendations. For each target, predesigned pools of four oligonucleotides were used and validated by Western blot analyses. For transfection of siRNA oligonu-

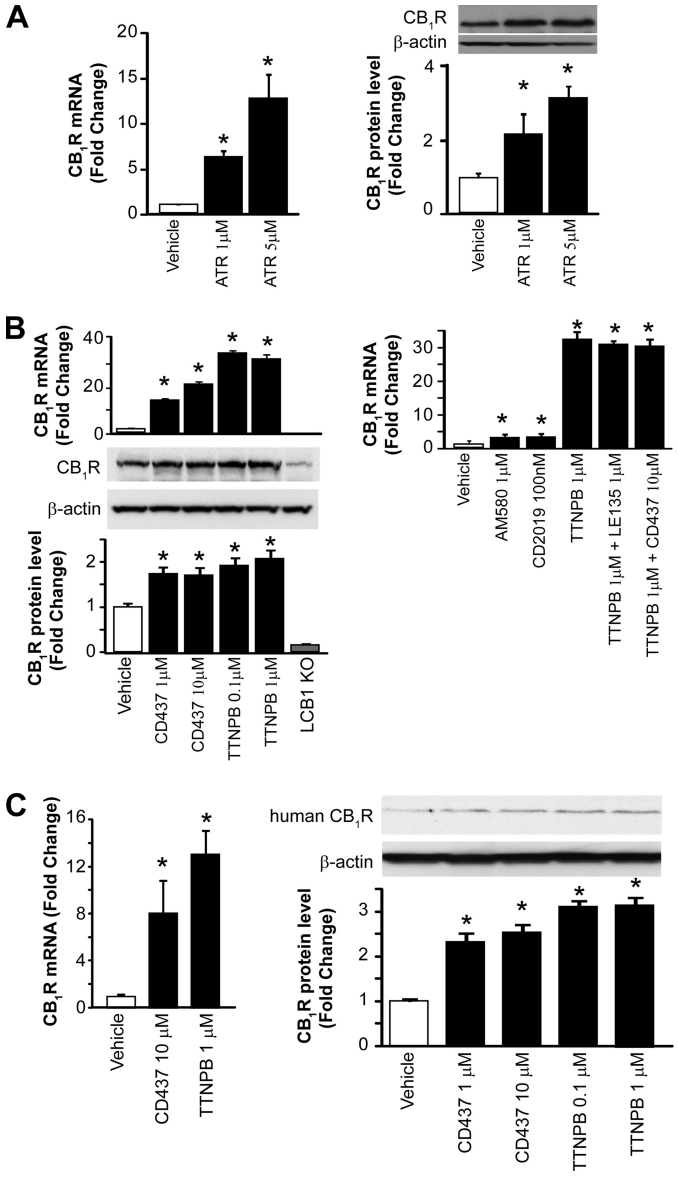

FIGURE 1. **RAR agonist-induced CB$_1$R expression in mouse and human hepatocytes.** *A*, hepatocytes were isolated from C57BL/6J mice and treated with all-*trans*-retinoic acid at the indicated concentration for 24 h. CB$_1$R mRNA expression was quantified by real-time PCR. *, $p < 0.05$ *versus* vehicle group, $n = 12$/group. CB$_1$R protein levels were determined by Western blot analysis followed by densitometric scanning. *B*, hepatocytes were treated with RAR panagonist TTNPB or RARγ agonist CD437 at the indicated concentration for 24 h. CB$_1$R mRNA expression was quantified by real-time PCR. *, $p < 0.05$ *versus* vehicle group, $n = 12$/group. CB$_1$R protein levels were determined by Western blot analysis followed by densitometric scanning. Hepatocytes from LCB$_1^{-/-}$ mice were used as negative control. *, $p < 0.05$ *versus* vehicle group, $n = 12$/group. *Right*, effects of 24-h incubations with RARα agonist AM580, RARβ agonist CD2019, the panagonist TTNPB alone, or TTNPB in the presence of RARβ antagonist LE135 or the RARγ agonist CD437 on CB$_1$R mRNA in hepatocytes (real-time PCR). *, $p < 0.05$ *versus* vehicle group, $n = 12$/group. *C*, hepatocytes obtained from human livers and treated with TTNPB or CD437 for 24 h. CB$_1$R expression was quantified by real-time PCR and Western blot. *, $p < 0.05$ *versus* vehicle group, $n = 4$/group. *Error bars*, S.E.

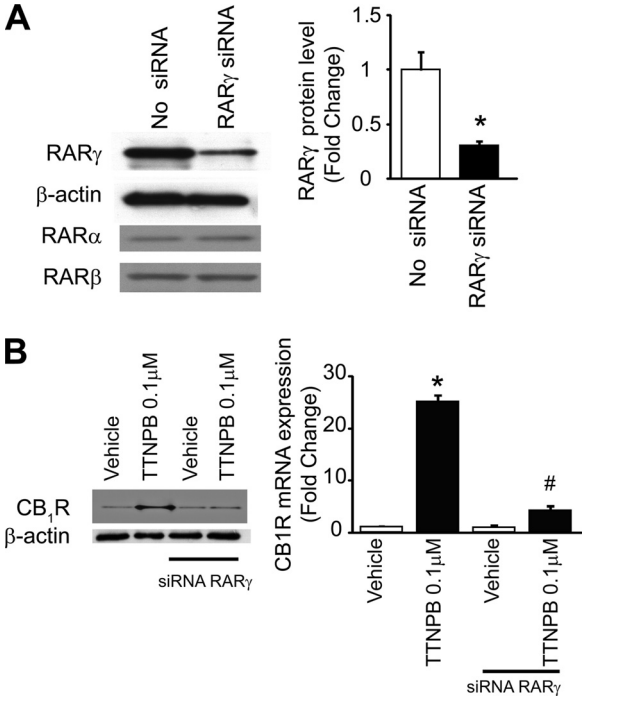

FIGURE 2. **RAR agonist-induced CB$_1$R expression is attenuated by siRNA-induced RARγ knock-down in mouse hepatocytes.** *A*, RARγ siRNA treatment of mouse hepatocytes results in selective knockdown of RARγ but not RARα or RARβ protein, as documented by Western blot. *, $p < 0.05$ *versus* vehicle group, $n = 4$/group. *B*, induction of hepatocyte CB$_1$R expression by RAR panagonist TTNPB is greatly attenuated by RARγ knockdown, as documented by Western blotting of immunoprecipitated protein and by real-time PCR. *, $p < 0.05$ *versus* vehicle group, $n = 6$/group. *Error bars*, S.E.

cleotides, hepatocytes were plated at 1×10^5 cells/well on 6-well culture plates and let sit overnight. The siRNA oligonucleotides were transfected the next day at a final concentration of 100 μM using Accell delivery medium. Three days following transfection, hepatocytes were collected and analyzed by real-time PCR and Western blotting. The Stealth RNAi negative control kit (Dharmacon) was used as a nonspecific transfection control.

Statistical Analyses—Results are reported as mean ± S.E. Statistical significance among groups was determined by one-way analysis of variance followed by *post hoc* Newman-Keuls analysis using GraphPad Prism 4.3 software. Probability values of $p < 0.05$ were considered significant. Statistical significance between two groups was determined by the two-tailed unpaired Student's *t* test. Correlations were determined by GraphPad Prism 4.3 software.

RESULTS

RAR Activation Induces CB$_1$R Expression in Hepatocytes—To test whether RA can regulate hepatic CB$_1$R expression, we incubated isolated mouse hepatocytes with all-*trans*-retinoic acid (24) and found that CB$_1$R mRNA and protein levels were increased significantly (Fig. 1*A*). RA can act via two types of retinoic acid receptors, RXR and RAR. We therefore tested the effect of the RXR agonist methoprene and the RAR panagonist TTNPB (25) on hepatocyte CB$_1$R mRNA levels. The RXR agonist was essentially ineffective (not shown), whereas TTNPB caused a robust, ~30-fold increase in CB$_1$R mRNA associated with a significant, ~2-fold increase in CB$_1$R protein at both 0.1 and 1 μM (Fig. 1*B*). To further test which RAR subtype is involved in this effect, we used selective RAR agonists. The RARγ agonist CD437 (26) caused a 14- and 21-fold increase in CB$_1$R mRNA at 1 and 10 μM, respectively, with parallel smaller increases in CB$_1$R protein, whereas the RARα agonist AM580

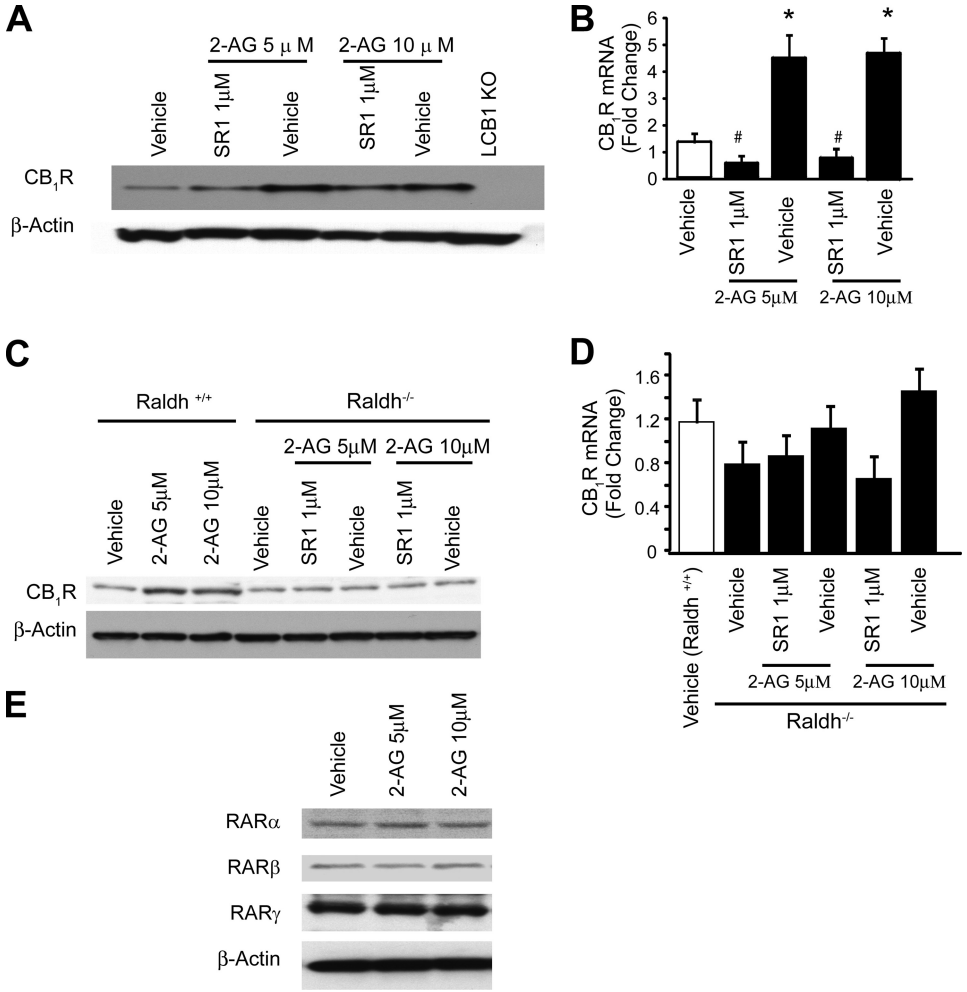

FIGURE 3. **2-AG induced, CB_1R-mediated CB_1R expression in mouse hepatocytes is reduced in hepatocytes from Raldh knock-out mice.** Hepatocytes from C57BL/6J mice were treated with 2-AG in the presence or absence of CB_1R antagonist SR141716 for 24 h. CB_1R protein was quantified by Western blotting after immunoprecipitation (*A*), whereas CB_1R mRNA expression was analyzed by real-time PCR (*B*). Hepatocytes from $Raldh^{+/+}$ and $Raldh^{-/-}$ mice were treated with 2-AG in the presence or absence of SR141716. CB_1R protein expression was analyzed by Western blot (*C*), and CB_1R mRNA expression was analyzed by real-time PCR (*D*). *, $p < 0.05$ *versus* vehicle group, $n = 12$/group. *E*, hepatocytes were isolated from C57BL/6J mice and treated with 2-AG for 24 h. RARα, RARβ, and RARγ protein expression were analyzed by Western blot. No changes were observed. *Error bars*, S.E.

(24) used at 1 μM and the RARβ agonist CD2019 (26) at 100 nM caused only a 2–3-fold increase in CB_1R mRNA (Fig. 1*B*, *right*) and no change in CB_1R protein (not shown). Moreover, the RARβ antagonist LE135 (27) at 1 μM did not affect the increase in CB_1R mRNA induced by TTNPB. Also, the combination of TTNPB and CD437 did not produce an additive effect, suggesting that they act via the same target (*i.e.* RARγ). Purified hepatocytes from liver-specific CB_1R knock-out ($LCB_1^{-/-}$) mice were used as negative control for CB_1R expression (Fig. 1*B*, *left panels*). The weak band observed may reflect trace nonspecific binding of the N-terminal antibody used because it could be eliminated when extracts were first immunoprecipitated and the precipitate was then blotted using another CB_1R antibody directed against the C terminus (see Fig. 3*A*). Parallel increases in CB_1R mRNA and protein were induced by CD437 and TTNPB in human primary cultured hepatocytes (Fig. 1*C*).

CB_1R Up-regulation by RAR Panagonist Is Attenuated by RARγ Knockdown in Hepatocytes—To further test the role of RARγ in the effects of various RAR agonists, RARγ expression in mouse hepatocytes was reduced by siRNA knockdown. siRNA treatment resulted in an ~80% reduction of RARγ mRNA, as verified by real-time PCR (not shown), as well as an ~75% reduction in RARγ protein levels, as documented by Western blotting (Fig. 2*A*), with no change in RARα and RARβ protein levels (Fig. 2*A*). The ability of the RAR panagonist TTNPB (1 μM) to induce CB_1R expression was reduced from a ~30-fold increase in mock-transfected hepatocytes to a 3–4-fold increase in cells with siRNA knockdown of RARγ (Fig. 2*B*). This indicates that up-regulation of hepatic CB_1R expression by RA and its analogs is mediated primarily via RARγ.

Activation of CB_1R by 2-AG Leads to Increased CB_1R Gene Expression in Hepatocytes—Ethanol feeding results in increased levels of 2-AG in HSC and an increase in CB_1R in hepatocytes, suggesting that 2-AG itself may be involved in regulating the expression of its own receptor. To test this, we have incubated primary cultured mouse hepatocytes with 5–10 μM 2-AG and found a dose-dependent increase in the expression CB_1R mRNA and protein, as detected by real-time PCR and Western blotting, respectively. This effect was largely prevented by simultaneous treatment with the CB_1R antagonist rimonabant (SR1; Fig. 3, *A* and *B*), indicating "feed-forward" autoregulation of CB_1R expression. This effect of 2-AG was absent in hepatocytes from retinaldehyde dehydrogenase-1 knock-out mice (Fig. 3, *C* and *D*), which are deficient in RA. Although this could suggest that induction of CB_1R expression by 2-AG requires RA, treatment with 2-AG did not alter the protein levels of RARα, -β, or -γ (Fig. 3*E*).

Both Ethanol Feeding and High Fat Diet Induce Fatty Liver and Up-regulate RARγ—Chronic exposure of 10–12-week-old male C57BL/6J mice to a low fat, liquid alcohol diet leads to hepatocellular damage, as reflected by increased plasma alanine aminotransferase and aspartate aminotransferase. Ethanol feeding, resulting in blood ethanol concentrations of 20.5 ± 6.0 mM, also leads to the development of fatty liver, as indicated by elevated hepatic levels of triglycerides with no change in hepatic cholesterol levels (Fig. 4*A*). Chronic ethanol feeding

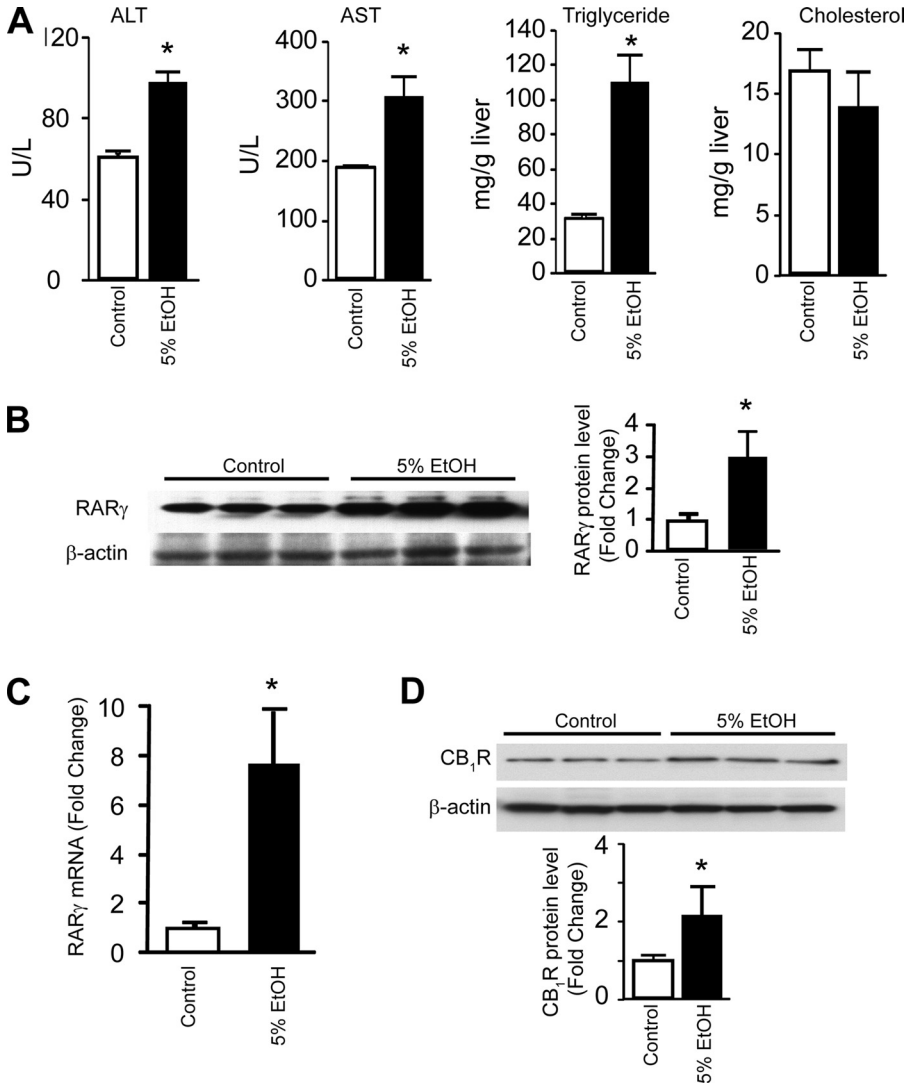

FIGURE 4. **Chronic alcohol diet induces liver damage in mice and up-regulates RARγ.** *A*, elevated serum levels of alanine aminotransferase, aspartate aminotransferase, and increase in hepatic triglycerides but no significant changes in hepatic cholesterol were observed in mice on ethanol diet. *B* and *C*, chronic alcohol diet results in increased hepatic RARγ protein (*B*) and mRNA levels (*C*), as quantified by Western blotting or real-time PCR, respectively. *, $p < 0.05$ *versus* vehicle group, $n = 6–12$/group. *D*, up-regulation of CB$_1$R protein level in hepatocytes C57BL/6J mice kept on liquid alcohol diet for 30 days. *U/L*, units/liter; *error bars*, S.E.

also results in a 7–8-fold increase of RARγ mRNA and an ~3-fold increase in RARγ protein level (Fig. 4, *B* and *C*), whereas RARα and RXR mRNA levels remain essentially unchanged (not shown). In agreement with earlier observations (1), the level of CB$_1$R protein was increased in alcohol-treated hepatocytes (Fig. 4*D*).

Fatty liver can also develop as a result of a high fat diet. Similar to the effect of chronic ethanol feeding, the expression of RARγ in hepatocytes was increased by a high fat diet relative to control chow (Fig. 5*A*). Although no such increase in RARγ was noted in 2-AG-treated hepatocytes (see above), the latter were treated *in vitro* for 24 h, as opposed to the chronic *in vivo* exposure to diet or alcohol. In agreement with earlier findings (3), high fat diet increased the expression of the lipogenic transcription factor SREBP-1c, its target fatty acid synthase, and CB$_1$R (Fig. 5).

Binding of RARγ to the CB$_1$R Gene Promoter—In view of the observed regulation of CB$_1$R by RARγ, we tested whether RARγ can bind to the CB$_1$R promoter. A CB$_1$R promoter fragment was generated by PCR using biotinylated primers spanning a 500-bp 5′ upstream region of the CB$_1$R gene. Using EMSA, nuclear extracts from vehicle-treated hepatocytes gave a shift in mobility, reflecting binding of unliganded RARγ to its DNA target (Fig. 6*A*), a phenomenon reported previously (28, 29). A further small shift was observed with extracts of agonist-pretreated hepatocytes, and as an indication of the specificity of the shifted complex, the presence of an RARγ antibody caused a supershift to a higher molecular weight position when nuclear extracts from CD437-treated cells were used (Fig. 6*A*). These findings demonstrate the interaction of RARγ with the CB$_1$R promoter. To further test the validity of this assay, it was replicated using recombinant RARγ replacing the nuclear extracts. RARγ was able to bind the CB$_1$R promoter element, and a supershift was observed with the RARγ antibody (Fig. 6*B*). In this latter case, the absence of the natural dimerization partner RXR may explain the reduced stability, suggested by the smear, and altered size of the complex.

RAR and RXR bind to target DNA in a sequence-specific manner. We therefore screened the 500-bp 5′ upstream region of the CB$_1$R gene that served as our EMSA probe, using the TFscan program with 1–2 mismatches. A target sequence of ~18 bp, located between −370 and −387, was identified by the search. When a PCR amplicon of 300 bp spanning the upstream region without the putative RARγ binding site was tested by EMSA, no shifts were observed with the fragment, which is compatible with the indicated sequence being the putative binding site (Fig. 6*C*). As a positive control in the same gel, the original probe did display a mobility shift and an antibody-induced supershift, which could be prevented by adding excess unlabeled probe to the assay mixture.

In Vivo Binding of RARγ to the CB$_1$R Promoter—The status of the RARγ transcription complexes present on the CB$_1$R promoters was determined using ChIP. Primary cultured hepatocytes were treated with vehicle or the RARγ agonists CD437 at 10 μM, TTNPB at 1 μM, or the endocannabinoid 2-AG at 10 μM. The presence of the CB$_1$R promoter in the chromatin immunoprecipitates was analyzed by semiquantitative PCR using specific primer pairs spanning the CB$_1$R pro-

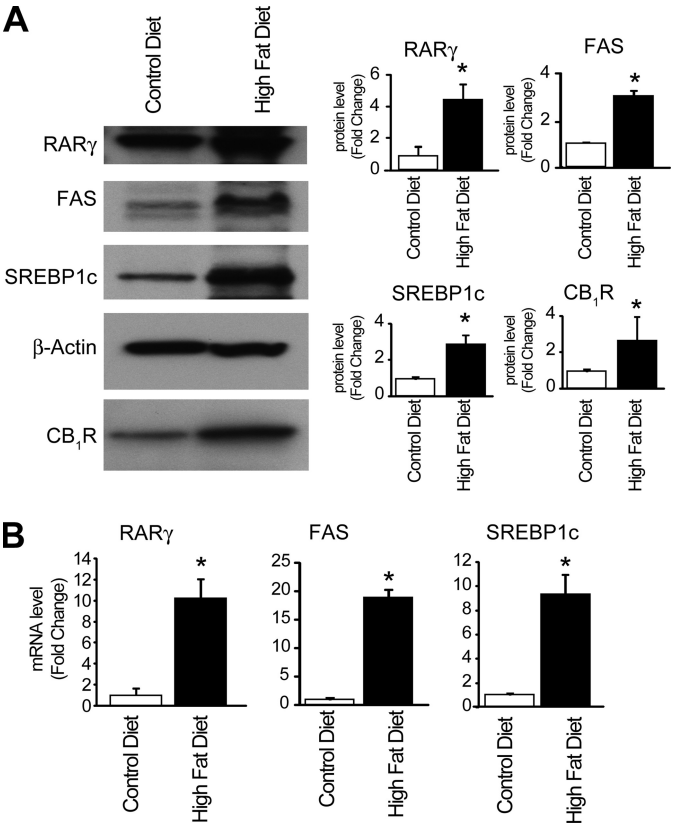

FIGURE 5. **High fat diet induces lipogenic gene expression in liver and up-regulates RARγ.** *A*, high fat diet results in increased hepatic levels of, RARγ, SREBP1, FAS, and CB_1R protein, as determined by Western blotting. *, $p < 0.05$ *versus* vehicle group, $n = 4$/group. *B*, high fat diet-induced increase in hepatic RARγ, SREBP1c, and FAS mRNA, as determined by real-time PCR. *, $p < 0.05$ *versus* vehicle group, $n = 12$/group.

moter −500 to +50 nucleotide region. We asked whether RAR agonists or 2-AG affected the recruitment of RARγ to the CB_1R promoter. As shown in Fig. 7*A*, chromatin immunoprecipitation with a monoclonal antibody against RARγ indicated that treatment with RAR agonists or 2-AG induced a significant increase in the occupancy by RARγ of the CB_1R gene promoter (*left*). Input DNA from each sample was also used as input control. To test for possible nonspecific binding of RARγ to other DNA regions and/or for genomic DNA contamination, primers for β-actin downstream genomic sequence were also used as a negative control for ChIP DNA (*right*). Real-time PCR analysis of ChIP enrichment showed a similar increase following 2-AG, CD437, and TTNPB treatments, and low level binding of RARγ to CB_1R promoter was also observed in the presence of vehicle only (Fig. 7*B*).

DISCUSSION

The present findings indicate that retinoic acid acting through RARγ is involved in the up-regulation of hepatic CB_1R observed in both alcohol- and high fat diet-induced fatty liver and may also be involved in mediating the autoinduction of CB_1R expression by endocannabinoids. In both alcohol-fed and high fat diet-fed mice, the hepatic expression of RARγ was significantly increased, which paralleled the increased hepatic expression of CB_1R in these conditions (30). Treatment of control hepatocytes by either a RAR panagonist or a selective RARγ agonist resulted in increased expression of CB_1R mRNA and protein, and the effect of the RAR panagonist was lost in cells with siRNA knockdown of RARγ. The dominant role of RARγ is further indicated by the lack of similar CB_1R induction by a RARα or a RARβ agonist, the inability of a RARβ antagonist to oppose the effect of the RAR pan-agonist, and the lack of additivity of the combination of the panagonist and RARγ agonist over the effect of the panagonist alone.

Although functional redundancies are known to exist among different subtypes of RAR and also between RAR and RXR, some of these redundancies may be artifactually generated in cells with gene knockouts (31). Indeed, it was earlier reported that only RARγ can mediate RA-induced differentiation of F9 and P19 embryonic cancer cells, with some input from RARα in the latter (31). RA-induced neuronal differentiation in P19 cells was associated with increased expression of CB_1R, but whether this was a direct action of RA or secondary to the process of neuronal differentiation was unclear. The present findings clearly demonstrate that RA acts as a direct transcriptional activator of non-neuronal CB_1R via RARγ.

Core consensus sequences of transcription factor binding sites, including an RAR element, have been mapped in the mouse CB_1R promoter (32). However, direct evidence for their role in transcriptional regulation has not been explored, with the exception of the STAT6 sequence S2, which was shown to be involved in the interleukin-4-inducible expression of CB_1R in T lymphocytes (33). Here we have provided strong evidence for the binding of liganded RARγ to a restricted, ~300-bp-long segment of the 5′ regulatory domain of the CB_1R gene. Although a perfect match for a *cis*-acting RARγ binding element is not present in this region, a DNA sequence element with two mismatches is a likely candidate as a RARγ recognition site. Additional evidence for the *in vivo* binding of RARγ to the CB_1R regulatory domain has been provided by the results of ChIP assays. Constitutive binding of RARγ to the CB_1R in the control sample was much lower than it was under *in vitro* conditions and could only be detected by real-time PCR (Fig. 7*B*). It is possible that under *in vivo* conditions, activation of membrane CB_1R generates a downstream signaling molecule that forms a complex with RARγ and stabilizes its binding to the promoter. Such an interaction, which remains to be explored, may be analogous to the recruitment of transcriptional co-regulators to target RA response elements through reversible interactions with RARs (34, 35).

A conspicuous finding is the striking difference between the robust, ~30-fold increase in CB_1R mRNA paralleled by a more modest, 3–4-fold increase in CB_1R protein by RARγ. Although we have not identified the specific mechanism underlying this difference, similar differences may result from the action of specific microRNAs that inhibit mRNA translation. Indeed, we were able to identify a conserved miR-128 binding site in the 3′-untranslated region of the mouse *Cnr1* gene (encoding CB_1R), using the TargetScan program. Validation of the functionality of this site will require further studies.

There is considerable evidence to suggest that activation of the endocannabinoid system, including increased expression of CB_1R in tissues involved in metabolic regulation, plays a key role in the development of diet-induced obesity

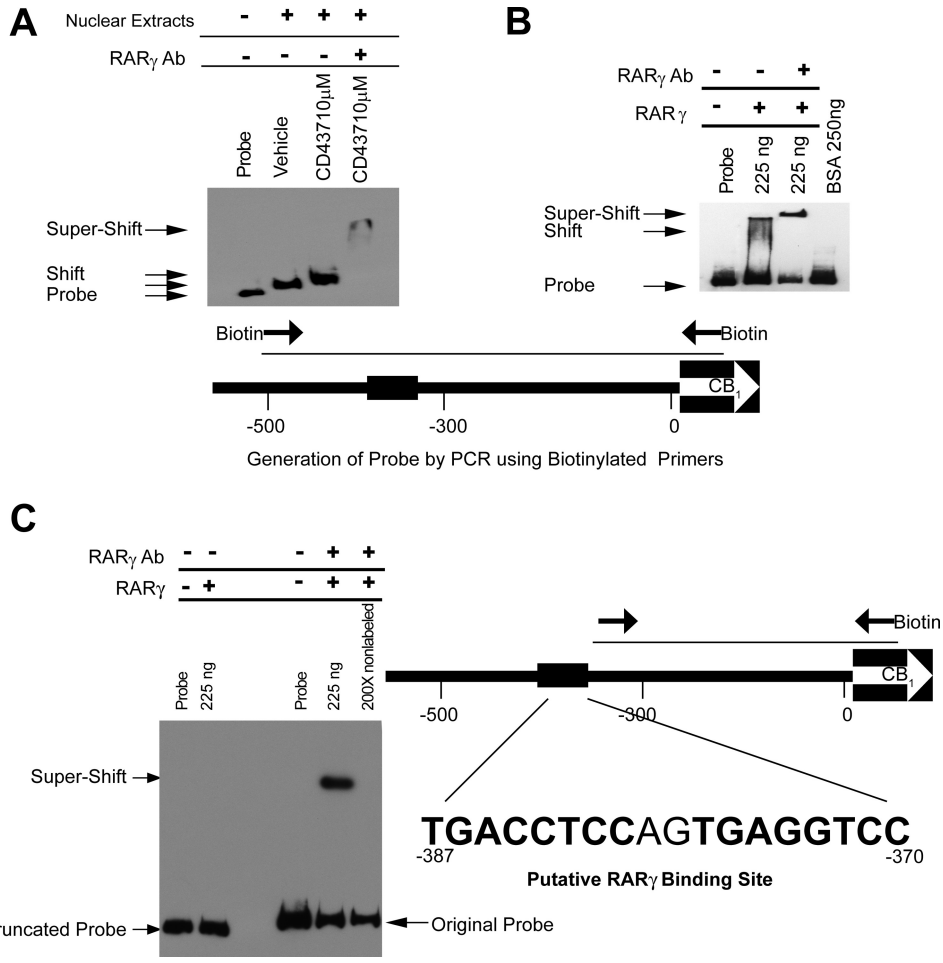

FIGURE 6. **RARγ binds to the CB_1R promoter region.** *A*, EMSA using a ~500-bp PCR fragment (see diagram) of the CB_1R promoter region with nuclear extracts of hepatocytes subjected to the indicated treatments. Note the slightly different shifts caused by unliganded *versus* liganded RARγ in *lanes 2* and *3*. Specificity of binding was demonstrated by supershift using RARγ monoclonal antibody (*lane 4*). Poly(dI-dC) was added to each reaction. *B*, CB_1R promoter/RARγ interaction using recombinant RARγ protein in the absence of RXR. The specificity of the binding was confirmed with supershift. Poly(dI-dC) was added to each reaction. *C*, a truncated, ~300-bp promoter fragment (see *diagram*) failed to bind the purified RARγ protein (*two left lanes*). In the same gel, binding of the original 500-bp probe to RARγ is demonstrated by antibody-induced supershift, which could be competed away by excess unlabeled probe. Nucleotide numbers are relative to the transcription initiation site of the mouse CB_1R. Poly(dI-dC) was added to each reaction. *Error bars*, S.E.

and hepatic steatosis as well as the associated hormonal/metabolic abnormalities, together called the metabolic syndrome. Increased tissue and plasma levels of endocannabinoids and a parallel increase in the expression of CB_1R in tissues critical to metabolic regulation, including skeletal muscle, liver, and adipose tissue, are suggestive of an overactive endocannabinoid system. This is further indicated by findings that chronic treatment with a CB_1R antagonist was able to reduce body weight, clear up fat from the liver, and improve the associated insulin resistance and dyslipidemias in animal models of obesity (36, 37) as well as in humans with obesity/metabolic syndrome (38, 39).

An additional interesting finding in the present study was the ability of the endocannabinoid 2-AG to up-regulate its own CB_1 receptor in hepatocytes. Although this effect was unexpected in view of the ability of high levels of cannabinoids to down-regulate CB_1 receptors in the brain, a mechanism of "desensitization" shared by many other ligand/receptor systems, a similar "autoinduction" of CB_1R by cannabinoids has been reported to occur in T lymphocytes, where the basal levels of CB_1R expression, similar to hepatocytes, are very low (40). More directly relevant to the present findings is a recent *in vivo* study in mice, which confirms the up-regulation of hepatic CB_1R by high fat diet and further reports its complete reversal by chronic treatment with a CB_1R antagonist (41). This suggests that the CB_1R autoinduction may also operate under *in vivo* conditions. The failure of 2-AG to induce CB_1R expression in hepatocytes from Raldh1 (retinaldehyde dehydrogenase-1) knock-out mice, which are deficient in RA, may suggest that RA is involved in the autoinduction of CB_1R. However, 2-AG was found not to affect cellular levels of RARγ, so the mechanism by which it increased the occupancy of the CB_1R promoter by RARγ, as documented by ChIP assays (Fig. 7*A*), remains unclear. A possible CB_1R-mediated increase in the cellular levels of RA, which could increase the fraction of ligand-bound RARγ, remains to be tested. CB_1R mRNA remained detectable in the liver of Raldh1 knock-out mice, which suggests that although RA and RARγ may be involved in the up-regulation of CB_1R, they are not required for its constitutive expression. The present findings also do not exclude the existence of additional, RARγ-independent mechanisms of regulation of CB_1R gene expression.

A link between the vitamin A/retinoic acid system and obesity and insulin resistance is suggested by recent findings that Raldh1-deficient mice are resistant to diet-induced obesity and glucose intolerance (5). This resistance has been attributed to the elevated tissue levels of retinaldehyde and its ability to inhibit adipogenesis by suppressing peroxisome proliferation-activated receptor γ and RXRα responses. Raldh1 knock-out mice are largely deficient in RA in the liver (14), and it is possible that at the greatly reduced hepatic RA levels, the high fat diet may have failed to induce CB_1R expression in tissues involved in metabolic control, and the resulting reduction in endocannabinoid "tone" may have contributed to the lean phenotype of these animals. Further experiments are under way to test this possibility.

Retinoic acid has been implicated in the control of a variety physiological processes, including cellular differentiation, tumor growth, and metabolic processes (42). The endocannabinoid system has also been implicated in many of these processes

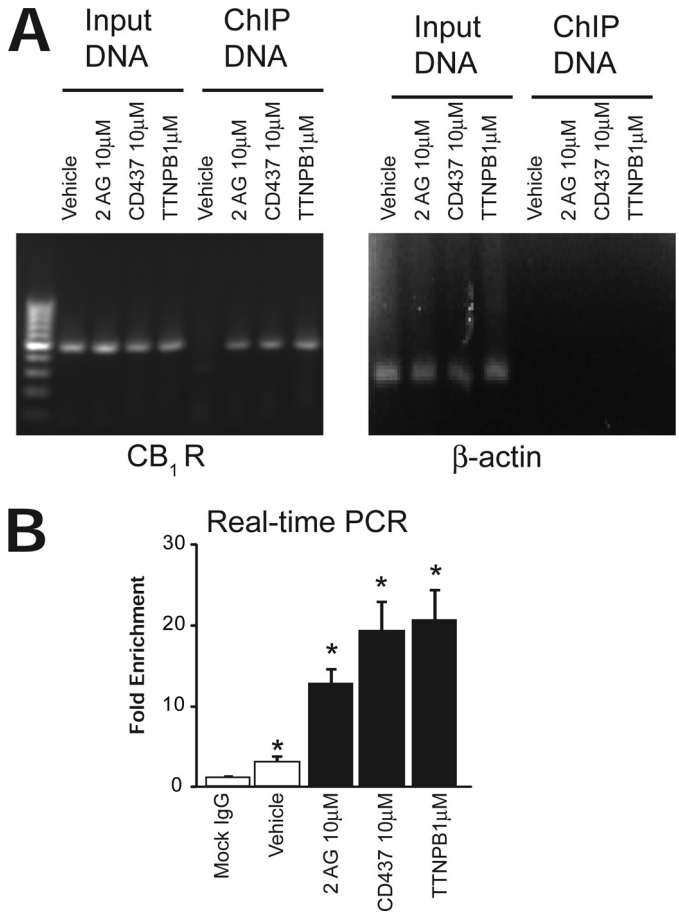

FIGURE 7. **Recruitment of RARγ and transactivation of CB_1R gene promoter by RARγ.** *A*, chromatin was extracted from isolated hepatocytes subjected to the indicated treatments, and ChIP assays with RARγ monoclonal antibody were performed. Anti-RARγ was used to immunoprecipitate a protein complex containing RARγ, as assayed by the DNA associated with this complex. Note the absence of RARγ in the complex from vehicle-treated cells and its presence in agonist-treated cells. The *input lane* confirms the comparable strength of the primer pairs specific for the promoter region. *B*, ChIP of RARγ followed by real-time PCR of CB_1R promoter using primers described in Table 1. Mock IgG was included as a control. Data are shown as -fold change *versus* input and are the average of three replicates ± S.E. (*error bars*).

(2), which could suggest that some of the pleiotropic actions of RA may be mediated via the endocannabinoid/CB_1 receptor system.

Acknowledgments—We thank Dr. A. Zimmer for originally providing the $CB_1^{+/-}$ heterozygote breeding pairs and Drs. B. Lutz and G. Marsicano for providing the CB_1R floxed mice used to generate the liver-specific knockouts. We also thank Dr. Q. Yuan for computational microRNA analyses.

REFERENCES

1. Jeong, W. I., Osei-Hyiaman, D., Park, O., Liu, J., Bátkai, S., Mukhopadhyay, P., Horiguchi, N., Harvey-White, J., Marsicano, G., Lutz, B., Gao, B., and Kunos, G. (2008) *Cell Metab.* **7,** 227–235
2. Pacher, P., Bátkai, S., and Kunos, G. (2006) *Pharmacol. Rev.* **58,** 389–462
3. Osei-Hyiaman, D., DePetrillo, M., Pacher, P., Liu, J., Radaeva, S., Bátkai, S., Harvey-White, J., Mackie, K., Offertáler, L., Wang, L., and Kunos, G. (2005) *J. Clin. Invest.* **115,** 1298–1305
4. Osei-Hyiaman, D., Liu, J., Zhou, L., Godlewski, G., Harvey-White, J., Jeong, W. I., Bátkai, S., Marsicano, G., Lutz, B., Buettner, C., and Kunos, G. (2008) *J. Clin. Invest.* **118,** 3160–3169
5. Ziouzenkova, O., Orasanu, G., Sharlach, M., Akiyama, T. E., Berger, J. P., Viereck, J., Hamilton, J. A., Tang, G., Dolnikowski, G. G., Vogel, S., Duester, G., and Plutzky, J. (2007) *Nat. Med.* **13,** 695–702
6. Duester, G. (2008) *Cell* **134,** 921–931
7. Gudas, L. J. (1994) *J. Biol. Chem.* **269,** 15399–15402
8. de Lera, A. R., Bourguet, W., Altucci, L., and Gronemeyer, H. (2007) *Nat. Rev. Drug Discov.* **6,** 811–820
9. Chambon, P. (1996) *FASEB J.* **10,** 940–954
10. Desreumaux, P., Dubuquoy, L., Nutten, S., Peuchmaur, M., Englaro, W., Schoonjans, K., Derijard, B., Desvergne, B., Wahli, W., Chambon, P., Leibowitz, M. D., Colombel, J. F., and Auwerx, J. (2001) *J. Exp. Med.* **193,** 827–838
11. Shulman, A. I., and Mangelsdorf, D. J. (2005) *N. Engl. J. Med.* **353,** 604–615
12. Svensson, A. C., Johansson, M., Persson, E., Carchenilla, M. S., and Jacobsson, S. O. (2006) *J. Neurosci. Res.* **83,** 1128–1140
13. Zimmer, A., Zimmer, A. M., Hohmann, A. G., Herkenham, M., and Bonner, T. I. (1999) *Proc. Natl. Acad. Sci. U.S.A.* **96,** 5780–5785
14. Fan, X., Molotkov, A., Manabe, S., Donmoyer, C. M., Deltour, L., Foglio, M. H., Cuenca, A. E., Blaner, W. S., Lipton, S. A., and Duester, G. (2003) *Mol. Cell. Biol.* **23,** 4637–4648
15. Marsicano, G., Goodenough, S., Monory, K., Hermann, H., Eder, M., Cannich, A., Azad, S. C., Cascio, M. G., Gutiérrez, S. O., van der Stelt, M., López-Rodriguez, M. L., Casanova, E., Schütz, G., Zieglgänsberger, W., Di Marzo, V., Behl, C., and Lutz, B. (2003) *Science* **302,** 84–88
16. Buettner, R., Parhofer, K. G., Woenckhaus, M., Wrede, C. E., Kunz-Schughart, L. A., Schölmerich, J., and Bollheimer, L. C. (2006) *J. Mol. Endocrinol.* **36,** 485–501
17. Bodor, A. L., Katona, I., Nyíri, G., Mackie, K., Ledent, C., Hájos, N., and Freund, T. F. (2005) *J. Neurosci.* **25,** 6845–6856
18. Sun, R., Jaruga, B., Kulkarni, S., Sun, H., and Gao, B. (2005) *Biochem. Biophys. Res. Commun.* **338,** 1943–1949
19. You, M., Matsumoto, M., Pacold, C. M., Cho, W. K., and Crabb, D. W. (2004) *Gastroenterology* **127,** 1798–1808
20. Schmittgen, T. D., and Livak, K. J. (2008) *Nat. Protoc.* **3,** 1101–1108
21. Mukhopadhyay, B., Marshall-Batty, K. R., Kim, B. D., O'Handley, D., and Nakai, H. (2003) *Mol. Microbiol.* **47,** 171–182
22. Shang, Y., Hu, X., DiRenzo, J., Lazar, M. A., and Brown, M. (2000) *Cell* **103,** 843–852
23. Verdel, A., Jia, S., Gerber, S., Sugiyama, T., Gygi, S., Grewal, S. I., and Moazed, D. (2004) *Science* **303,** 672–676
24. Shimada, T., Ross, A. C., Muccio, D. D., Brouillette, W. J., and Shealy, Y. F. (1997) *Arch. Biochem. Biophys.* **344,** 220–227
25. Alique, M., Lucio-Cazaña, F. J., Moreno, V., Xu, Q., Konta, T., Nakayama, K., Furusu, A., Sepulveda, J. C., and Kitamura, M. (2007) *Pharmacology* **79,** 57–64
26. Falanga, A., Consonni, R., Marchetti, M., Locatelli, G., Garattini, E., Passerini, C. G., Gordon, S. G., and Barbui, T. (1998) *Blood* **92,** 143–151
27. Li, Y., Hashimoto, Y., Agadir, A., Kagechika, H., and Zhang, X. (1999) *J. Biol. Chem.* **274,** 15360–15366
28. Hauksdottir, H., Farboud, B., and Privalsky, M. L. (2003) *Mol. Endocrinol.* **17,** 373–385
29. Gillespie, R. F., and Gudas, L. J. (2007) *J. Biol. Chem.* **282,** 33421–33434
30. Osei-Hyiaman, D., Depetrillo, M., Harvey-White, J., Bannon, A. W., Cravatt, B. F., Kuhar, M. J., Mackie, K., Palkovits, M., and Kunos, G. (2005) *Neuroendocrinology* **81,** 273–282
31. Taneja, R., Roy, B., Plassat, J. L., Zusi, C. F., Ostrowski, J., Reczek, P. R., and Chambon, P. (1996) *Proc. Natl. Acad. Sci. U.S.A.* **93,** 6197–6202
32. McCaw, E. A., Hu, H., Gomez, G. T., Hebb, A. L., Kelly, M. E., and Denovan-Wright, E. M. (2004) *Eur. J. Biochem.* **271,** 4909–4920
33. Börner, C., Bedini, A., Höllt, V., and Kraus, J. (2008) *Mol. Pharmacol.* **73,** 1013–1019
34. Gillespie, R. F., and Gudas, L. J. (2007) *J. Mol. Biol.* **372,** 298–316
35. Epping, M. T., Wang, L., Edel, M. J., Carlée, L., Hernandez, M., and Bernards, R. (2005) *Cell* **122,** 835–847
36. Poirier, B., Bidouard, J. P., Cadrouvele, C., Marniquet, X., Staels, B., O'Connor, S. E., Janiak, P., and Herbert, J. M. (2005) *Diabetes Obes. Metab.*

7, 65–72
37. Gary-Bobo, M., Elachouri, G., Gallas, J. F., Janiak, P., Marini, P., Ravinet-Trillou, C., Chabbert, M., Cruccioli, N., Pfersdorff, C., Roque, C., Arnone, M., Croci, T., Soubrié, P., Oury-Donat, F., Maffrand, J. P., Scatton, B., Lacheretz, F., Le Fur, G., Herbert, J. M., and Bensaid, M. (2007) *Hepatology* **46,** 122–129
38. Després, J. P., Golay, A., and Sjöström, L. (2005) *N. Engl. J. Med.* **353,** 2121–2134
39. Pi-Sunyer, F. X., Aronne, L. J., Heshmati, H. M., Devin, J., and Rosenstock, J. (2006) *JAMA* **295,** 761–775
40. Börner, C., Höllt, V., Sebald, W., and Kraus, J. (2007) *J. Leukoc. Biol.* **81,** 336–343
41. Jourdan, T., Djaouti, L., Demizieux, L., Gresti, J., Vergès, B., and Degrace, P. (2010) *Diabetes* **59,** 926–934
42. Altucci, L., Leibowitz, M. D., Ogilvie, K. M., de Lera, A. R., and Gronemeyer, H. (2007) *Nat. Rev. Drug Discov.* **6,** 793–810